

## AMELIORATION OF PLASMA-MATERIAL INTERACTIONS AND IMPROVEMENT OF PLASMA PERFORMANCE WITH A FLOWING LIQUID LI LIMITER AND LI CONDITIONING ON EAST

R. Maingi<sup>1</sup>, J.S. Hu<sup>2</sup>, G.Z. Zuo<sup>2</sup>, D. Andruczyk<sup>3</sup>, J.M. Canik<sup>4</sup>, A. Diallo<sup>1</sup>, K.F. Gan<sup>5</sup>, E. Gilson<sup>1</sup>, X.Z. Gong<sup>2</sup>, T.K. Gray<sup>4</sup>, M. Huang<sup>2</sup>, R. Lunsford<sup>1</sup>, D.K. Mansfield<sup>1</sup>, X. C. Meng<sup>6</sup>, T.H. Osborne<sup>7</sup>, D.N. Ruzic<sup>3</sup>, Z. Sun<sup>2</sup>, K. Tritz<sup>8</sup>, W. Xu<sup>2</sup>, Z. Wang<sup>9</sup>, B.D. Wirth<sup>9</sup>, K. Woller<sup>10</sup>, S.J. Zinkle<sup>9</sup>, and the EAST Team

<sup>1</sup> Princeton Plasma Physics Laboratory, 100 Stellarator Road, Princeton, NJ 08540, USA

<sup>2</sup> Institute of Plasma Physics, Chinese Academy of Sciences, Hefei, Anhui 230031, China

<sup>3</sup> University of Illinois, Urbana-Champaign, Champaign IL 61820, USA

<sup>4</sup> Oak Ridge National Laboratory Oak Ridge, TN 37830 USA

<sup>5</sup> University of Tennessee, Knoxville TN 37996, USA

<sup>6</sup> Department of Applied Physics, Hunan University, Changsha 410082, China

<sup>7</sup> General Atomics, San Diego, CA 92121, USA

<sup>8</sup> Johns Hopkins University, Baltimore MD 21211, USA

<sup>9</sup> Los Alamos National Laboratory, Los Alamos NM 87545, USA

<sup>10</sup> Massachusetts Institute of Technology, Cambridge MA 02139, USA

Emails: [rmaingi@pppl.gov](mailto:rmaingi@pppl.gov), [hujs@ipp.ac.cn](mailto:hujs@ipp.ac.cn) (the first two authors are equal co-authors)

### Abstract

The use of lithium conditioning with multiple techniques, i.e. flowing liquid lithium limiters and lithium injection, has contributed to the achievement of H-mode discharges with greater than 100 s pulse length; new results are described from several of these techniques. First new results from two designs of a midplane flowing liquid lithium limiter and associated experiments in EAST are presented, comparing against the first generation results. Generation 2 used the same stainless steel-coated copper heat sink as used in Generation 1, with a thicker stainless steel protective layer, while Gen. 3 was fabricated from solid TZM, a molybdenum alloy. Gen. 2 and 3 were exposed to higher current plasmas and substantially higher auxiliary heating power than Generation 1, and plasma performance was generally improved. In addition ELM elimination was achieved with the use of real-time lithium injection in discharges that used the upper tungsten divertor, extending previous results with the lower carbon divertor. A marked reduction in the W sputtering source was also observed with Li powder injection. Finally the ability of lithium granules to trigger and pace ELMs is documented, along with the observation of a critical granule size threshold for ELM triggering as conceptually predicted by theory.

### 1. INTRODUCTION

A main goal of the Experimental Advanced Superconducting Tokamak (EAST) is to demonstrate long-pulse high performance H-mode discharges while testing science and technology issues for ITER and the design of the Chinese Fusion Engineering Test Reactor (CFETR)<sup>1</sup>. The EAST device has auxiliary heating from neutral beams ( $\leq 10$  MW), lower hybrid heating and current drive ( $\leq 3$  MW), electron cyclotron heating ( $\leq 2$  MW), and ion cyclotron resonant frequency heating ( $\leq 3$  MW). The lower divertor plasma-facing components (PFCs) are made of carbon, the upper divertor of ITER-like tungsten (W) monoblock, and the central column of TZM, a molybdenum alloy.

H-mode discharge duration continues to grow in EAST, from the recently published 60 second discharges<sup>2</sup> to ones exceeding 100 s<sup>3</sup>. Wall conditioning has played a crucial role in enabling access to long pulses<sup>4</sup>. EAST relies on extensive wall conditioning via lithium (Li) evaporation and real-time Li powder injection. Additionally, Li granule injection is used for edge-localized mode (ELM) triggering studies and a midplane-inserted flowing liquid Li limiter (FLiLi) aims to mitigate plasma-material interactions (PMI). This paper presents new results since the last IAEA conference from this range of Li delivery techniques, emphasizing the flowing liquid Li limiter results.

## 2. FLOWING LIQUID LITHIUM LIMITER EXPERIMENTS

Due to its strong chemical reactivity with vacuum impurity gases, maintaining a clean Li plasma-facing surface for hydrogen pumping requires continuous flow for long pulse discharges, a key purpose of the flowing liquid Li (FLiLi) limiter program in EAST<sup>5-7</sup>. Three generations of limiters have now been exposed to EAST H-mode plasmas. [Table 1](#) compares their design characteristics, and the types of plasmas exposed to them.

**Table 1:** Comparison of three generations of the FLiLi limiter

Generation	Heat Sink	SS thickness (mm)	JxB pumps	Max. $P_{aux}$ (MW)	Max. $q_{exh}$ (MW/m <sup>2</sup> )	Max. $W_{MHD}$ (kJ)
1	Cu + SS	0.1	1	1.9	3.5	120
2	Cu + SS	0.5	2	4.5	4	170
3	Mo (TZM)	NA	2	8.3	TBD	280

The first generation FLiLi limiter<sup>8, 9</sup> consisted of a plate made of copper (Cu), due to its high thermal conductivity, covered with a 0.1mm thick layer of stainless steel to prevent Li-Cu reactions. A stainless steel distributor with small holes was attached to the top of the plate, while a stainless steel collector was affixed to the bottom. A  $j \times B$  magnetic pump drove the liquid lithium from the collector to the distributor, while flow down the limiter surface was gravity-driven. Plate-embedded heaters maintained a minimum temperature above the Li melting point of 180.5 °C, and inlet and outlet tubes were attached to the back of the limiter for He gas cooling. Li was loaded into the FLiLi limiter via a transfer box, and the limiter assembly was inserted into EAST on the Material And Plasma Evaluation System (MAPES) apparatus. To summarize the first results: the FLiLi limiter was compatible with RF-heated H-modes, even when placed within 1 cm of the separatrix, and modest improvements in plasma performance were observed. During times of strong PMI, intense green light emission from the plasma indicative of singly charged Li ions was observed, qualitatively similar to plasma emission during Li powder injection<sup>5, 6</sup>. Inspection of the limiter after exposure revealed marked damage on the right side of the limiter (ion drift side), due to PMI. In particular localized regions where the stainless steel coating had been removed and Li interacted with the underlying copper were evident ([Fig. 2d](#)). In addition the distributor developed a large crack that connected the small hole, preventing uniform flow along the surface.

A 2<sup>nd</sup> generation flowing liquid Li limiter ([Fig. 1](#)) was designed with several upgrades<sup>10</sup> to prevent the damage observed in the 1<sup>st</sup> generation system.

First a thicker stainless steel protective layer (0.5mm vs. 0.1 mm) was used to prevent PMI from exposing the Cu heat sink to the liquid Li. Next an additional  $j \times B$  magnetic pump was added for a more uniform supply of Li to the distributor on the top of the limiter. In addition, surface texturing was implemented in the 2<sup>nd</sup> generation, which improved the wetting uniformity of the liquid Li flowing on the front face. Also, an improved method for manufacturing the top Li distributor from two pieces was developed; this new design avoided the crack that developed during deployment of the 1<sup>st</sup> generation distributor. This limiter was found to be compatible with H-mode plasmas, even when placed within 1 cm of the separatrix in RF heated discharges<sup>10</sup>.

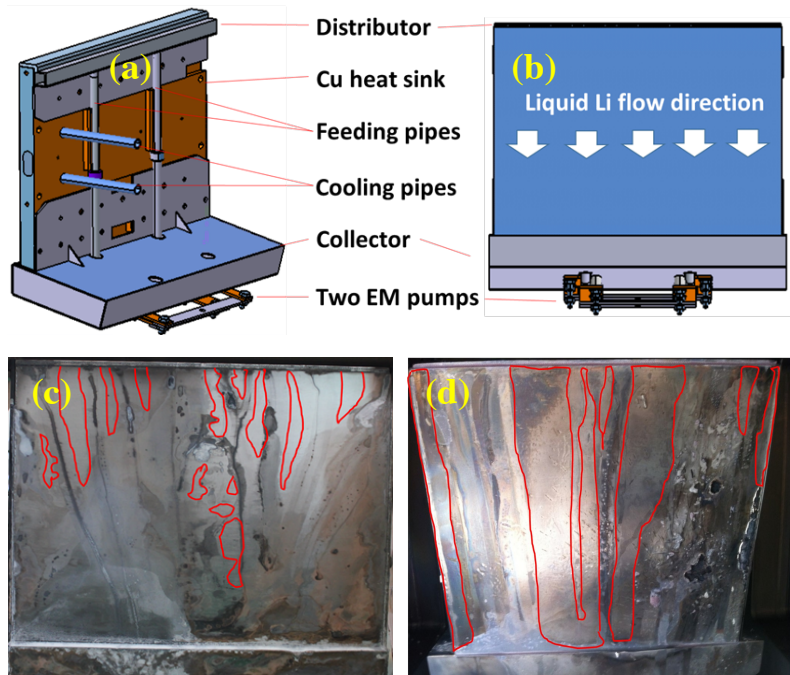


**Fig. 1:** (a) schematic of back side of 2<sup>nd</sup> generation FLiLi plate, (b) front side; comparison of (c) 2<sup>nd</sup> (12/16) and (d) 1<sup>st</sup> (10/14) generation flowing liquid Li plate after plasma exposure.

The 2<sup>nd</sup> generation limiter was inserted into plasma discharges on two separate dates<sup>11</sup>, demonstrating an ability to restart Li flow after it has been stopped for more than a week. Camera images after the first exposure showed a relatively pristine limiter surface, but photographs after the second exposure showed streaks on the plasma-facing surface, indicating the formation of surface-contaminating compounds that may have hindered free flow in the second exposure. Fig. 1 also compares the limiter plate condition after plasma exposure for the 2<sup>nd</sup> generation (panel 1c – no visible damage) and the 1<sup>st</sup> generation limiters (panel 1d – visible damage on the right hand side of the limiter face)<sup>7, 10</sup>. In addition the fractional surface area that was un-wetted (red outlines) by the Li was < 20% in 1c, vs. ~70% in 1d.

Fig. 2 shows that the upper divertor  $D_\alpha$  emission and ELM size were continuously reduced in otherwise constant discharge conditions into which the 2<sup>nd</sup> generation limiter was inserted<sup>11</sup>: plasma current  $I_p = 0.45$  MA, toroidal field  $B_t = -2.5$  T,  $P_{aux} = 2.9$  MW, in an upper single-null configuration with ion grad-B drift toward the lower divertor. These results showing progressive conditioning and ELM mitigation are qualitatively similar to Li powder injection on EAST<sup>12</sup>, as well as with pre-discharge Li evaporation in NSTX<sup>13</sup>. Finally, short-lived *true* ELM-free phases (and also ohmic H-modes) were observed for the first time in EAST with increasing  $\tau_E$  and transient  $H_{H98y2} \leq 2$  when the 2<sup>nd</sup> generation limiter was inserted (visible around e.g.  $t = 3.2$  s in Fig. 2d). We refer to these as *true* ELM-free H-modes because of the density accumulation observed, which is not seen in the ELM eliminated cases observed with e.g. real-time Li powder injection.

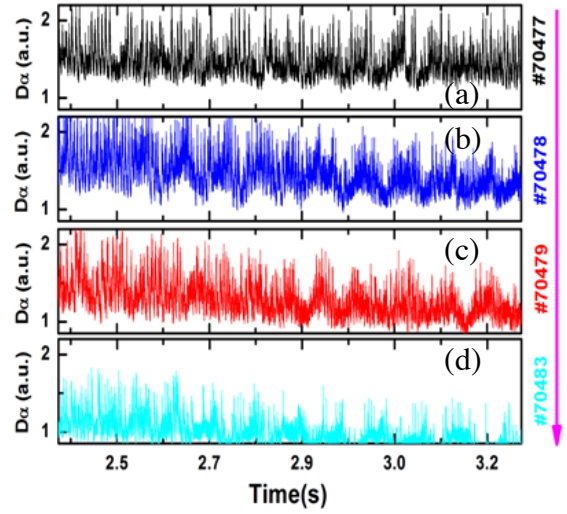


Fig. 2:  $D_\alpha$  emission in discharges with FLiLi inserted within 1 cm of separatrix, showing progressively reduced recycling.

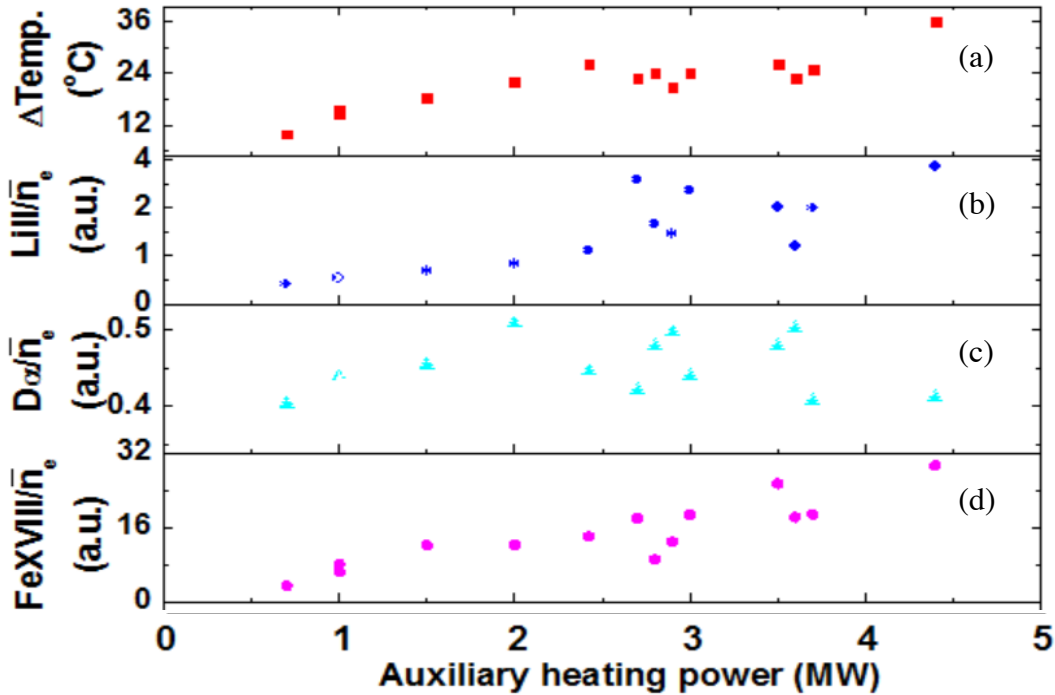
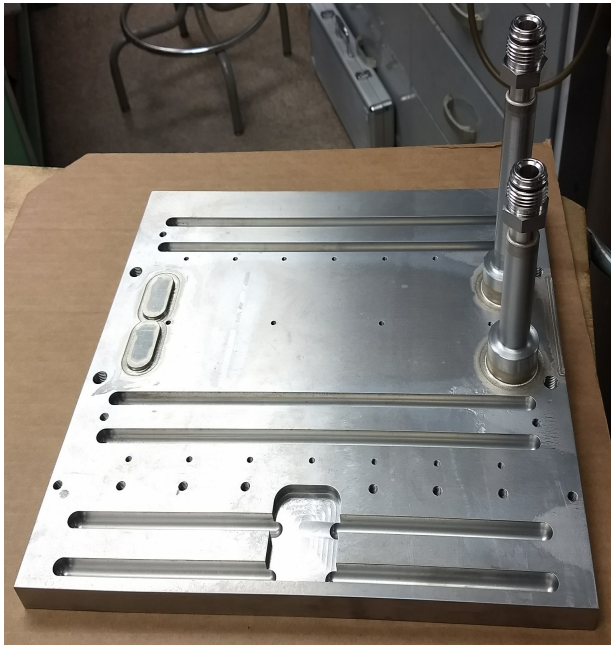


Fig. 3: Performance of 2<sup>nd</sup> generation limiter and plasma emission vs. auxiliary heating power  $P_{aux}$ : (a) limiter temperature rise, (b) Li-II emission, (c)  $D_\alpha$  emission, and (d) Fe-XVIII emission, normalized by line-average density.

The performance of the limiter and plasma characteristics is shown as a function of increasing auxiliary power<sup>11</sup> in Fig. 3. It can be seen that the limiter temperature rise from near-surface thermocouples, the plasma Li-II emission, and the Fe-XV emission all increase with increasing  $P_{aux}$ . The increasing Fe emission, likely from PMI with dry spots on the limiter surface, and/or with the distributor or collector, motivated use of a substrate more resistant to sputtering, e.g. W or Mo. Using a 1-D infinite slab thermal conduction model, we computed from the thermocouple temperature rise that a peak heat flux  $\sim 4 \text{ MW/m}^2$  was exhausted by the 2<sup>nd</sup> generation FLiLi in the discharge with  $P_{aux} \sim 4.5 \text{ MW}$ <sup>11</sup>.

Due to the progressive successes of the FLiLi limiter program, a 3<sup>rd</sup> generation limiter constructed entirely of TZM, an alloy with  $> 99\%$  Mo, was fabricated by conventional manufacturing techniques. Mo was chosen due to its higher sputtering resistance, as compared to stainless steel, and its compatibility with conventional manufacturing, as compared to tungsten. Fig. 4 shows a picture of the back side of the limiter, including the grooves for insertion of Li-compatible cartridge heaters, and inlet and outlet Mo tubes for steady state cooling by flowing He gas. The end connectors are Swagelok fittings, designed to accommodate stainless steel pipes to and from the He supply bottle. The front face of this limiter is smooth, polished for a mirror-like finish to facilitate easy wetting. Two plates were manufactured: one for insertion into EAST, and one for testing in the HIDRA device<sup>14</sup> at the Univ. of Illinois (UI-UC). In addition to the flat plate shown, a version also made out of



*Fig. 4: Picture of the back-side of the 3<sup>rd</sup> generation limiter plate made of TZM, showing grooves for the embedded heaters, inlet and outlet tubes for He cooling, and various holes for mounting to the EAST Li Plasma Evaluation System.*

TZM with trenches is being fabricated at UI-UC to augment the gravity-driven flow with thermoelectric MHD driven flow; this design is referred to as liquid metal infused trenches (LIMIT)<sup>15</sup>.

The 3<sup>rd</sup> generation FLiLi was inserted into the edge of EAST H-mode plasmas in an upper single-null configuration with ion grad-B drift toward the upper divertor; preliminary results from this experiments are reported here. Fig. 5 compares a reference discharge (black) with one in which the FLiLi limiter was inserted to within 3 cm of the separatrix (red) with  $I_p = 0.55 \text{ MA}$ ,  $B_t = 2.5 \text{ T}$ ,  $P_{aux} = 7.9\text{-}8.3 \text{ MW}$ , EM pump current = 100 A. The neutral Li line emission is higher with the limiter inserted, as expected, while the  $D_\alpha$  emission from the upper divertor is substantially lower. The stored energy is slightly higher with the limiter inserted, though this is partly due to modestly higher heating power. The line-average density is comparable. Overall the limiter performed well for this set of discharges. Upon removal, however, damage to the electron drift side of the limiter plate was evident, as was damage to the right hand side of the collector. The reasons for the damage are being investigated.

### 3. LITHIUM POWDER AND GRANULE INJECTION EXPERIMENTS

As mentioned above, EAST relies on extensive wall conditioning via Li evaporation and real-time powder injection<sup>16</sup>. In previous experiments, Li powder injected into the lower-single null shape with carbon PFCs eliminated ELMs in long pulse EAST H-modes<sup>17</sup>. However no strong pedestal modification was observed when Li pellets were injected into high-power H-modes in ASDEX-Upgrade, which uses all W PFCs<sup>18</sup>, raising the question of whether Li seeding could work at all with high-Z PFCs.

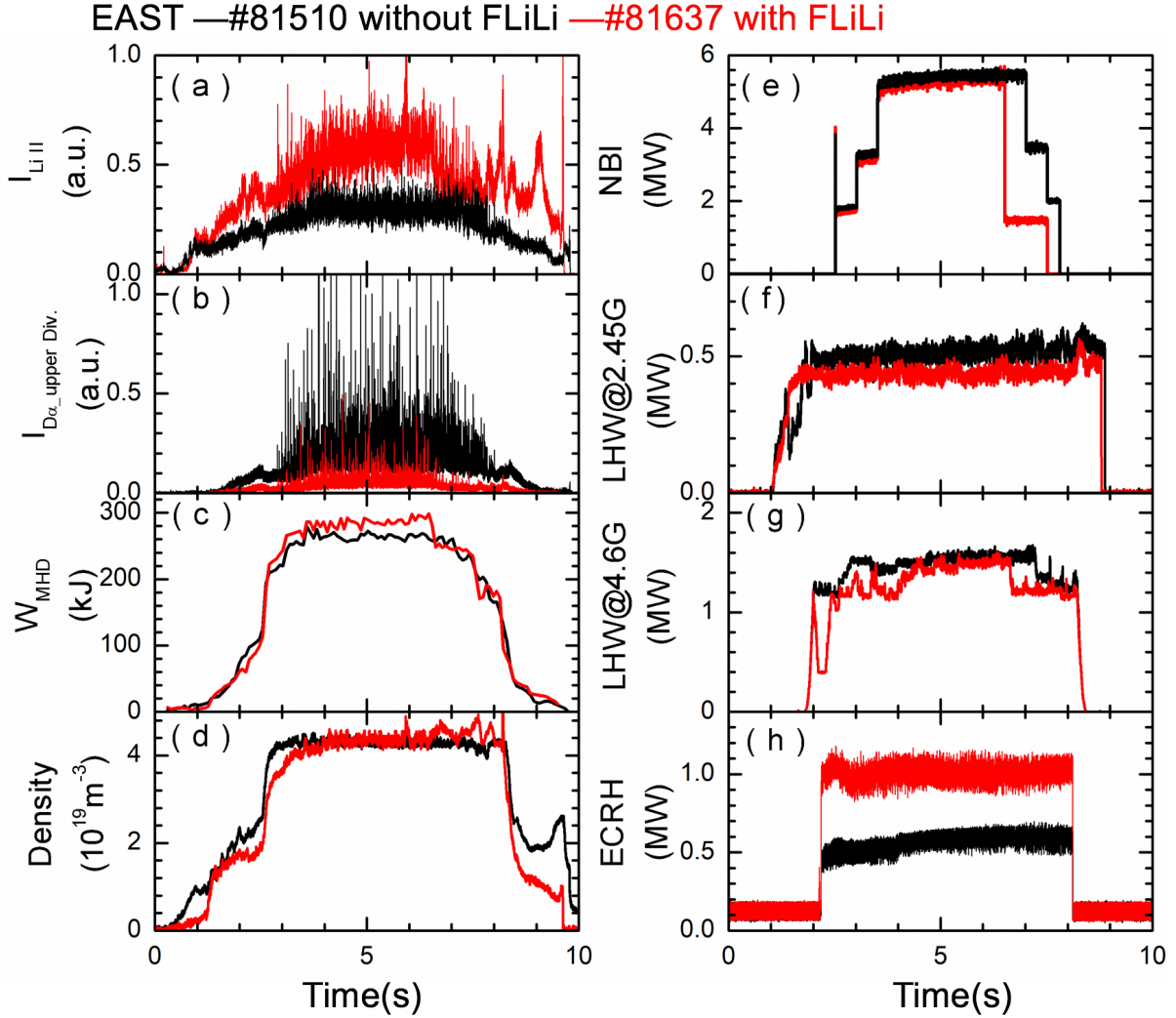


*Fig. 5: Comparison of plasma with (red - #81637) and without (black-#81510) the 3<sup>rd</sup> generation FLiLi limiter inserted: (a) Li-II emission, (b) Upper divertor  $D_\alpha$  emission, and (c) Plasma stored energy, (d) line-average density, (e) neutral beam injected power, (f) low frequency lower hybrid power, (g) high frequency lower hybrid power, and (h) electron cyclotron resonant heating power. The auxiliary heating power with FLiLi was 6% higher, partly resulting in higher stored energy.*

To assess this question, Li powder was injected into upper-single null H-modes in EAST that used the ITER-like W monoblock divertor, and ELMs were successfully eliminated<sup>12</sup>. Fig. 6a shows the upper-single null equilibrium along with the two Li dropper poloidal locations. Fig. 6b and 6c show the plasma light emission without and with Li powder injection: the typical green light due to Li-II emission is clearly observed. The discharge parameters were  $I_p = 0.4$  MA,  $B_t = -2.5$ T,  $P_{aux} = 2.7$  MW, and ion grad-B drift toward the lower divertor. Li powder was injected from  $t = 3.5$ -8 sec. Fig. 6d shows ELMs in the reference discharge, with complete ELM elimination evident in the discharge with the real-time Li injection in Fig. 6e. Note that the two discharges just before #70593 showed ELM elimination from  $t = 5$ -8 s and  $t = 3.8$ -5 s respectively. Thus at constant Li injection rates, the ELM elimination became progressively easier and of longer duration. A few ELMs appeared to be triggered by the NBI short pulses for charge exchange recombination measurements in the two intervening discharges #70591 and #70592; these short NB pulses were eliminated for the discharge in Fig. 6e. The baseline  $D_\alpha$  emission was also reduced, indicating a cumulative wall conditioning effect of the Li injection. Data-constrained edge transport modeling with the SOLPS code indicated a cumulative reduction of the recycling coefficient by about 20%<sup>19</sup>. The edge  $n_e$  and  $T_e$  profiles were unchanged to within measurement accuracy, while the global energy confinement was reduced by up to 10%. Nonetheless the  $H_{H98y2}$  was maintained at about 1.2, well above the previous ELM suppression with Li injection on the lower carbon divertor with  $H_{H98y2} \sim 0.75$ <sup>17</sup>. Furthermore these results provide an existence proof of ELM elimination with tungsten PFCs, something that was not observed with Li pellet injection into the core of ASDEX-Upgrade<sup>18</sup>.

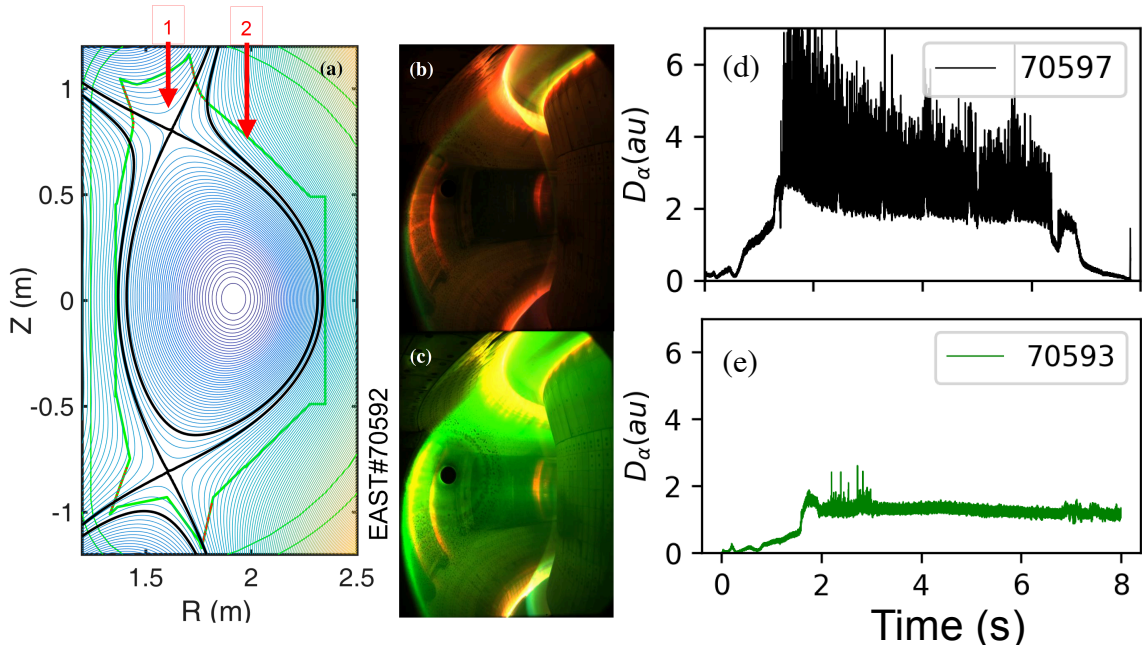


*Fig. 6: Use of Li powder dropper in the upper tungsten divertor in EAST: (a) equilibrium showing two injection locations, (b) visible color camera emission before and (c) after Li powder injection;  $D_\alpha$  emission in (d) reference discharge no powder, and (e) discharge with powder injection, showing ELM elimination.*

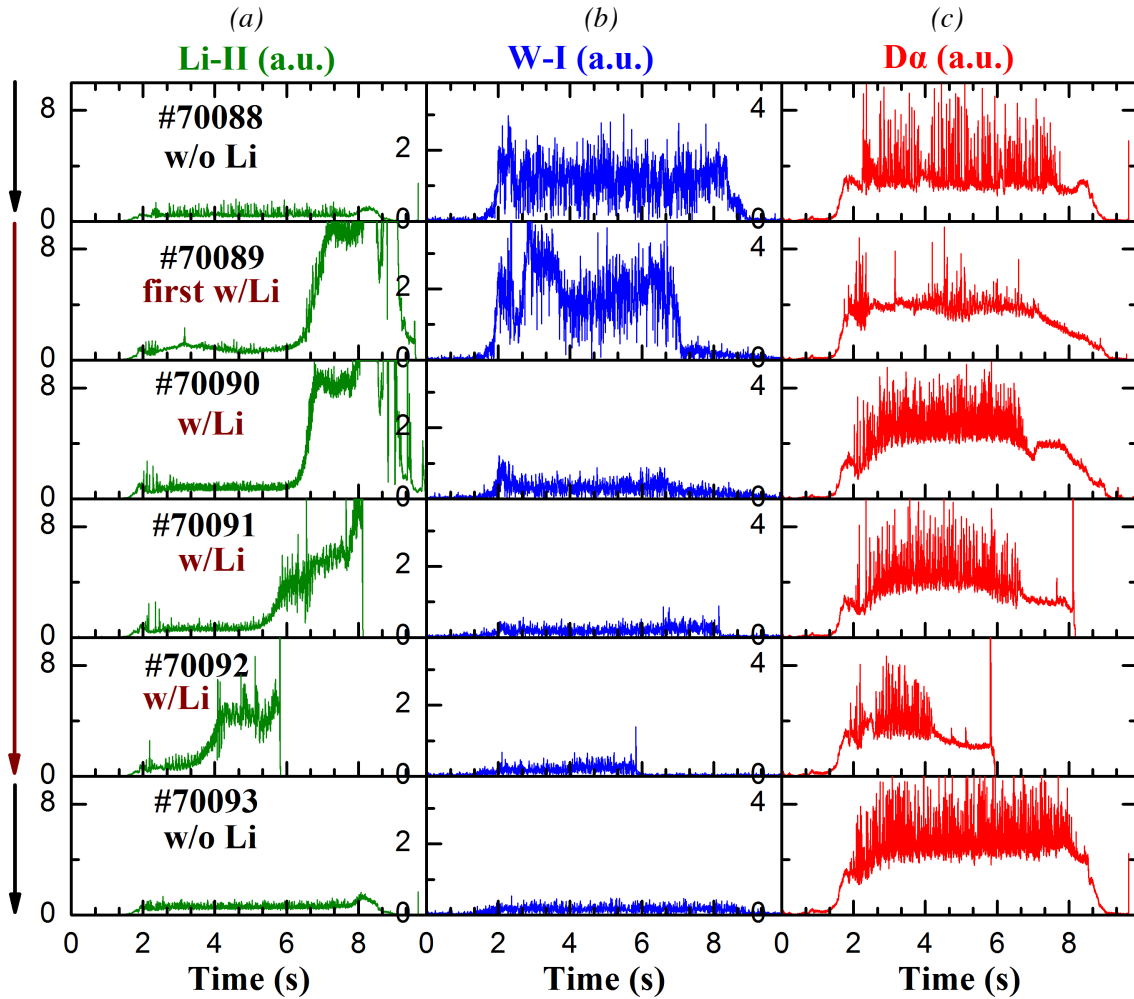


*Fig. 7: Evolution of various plasma emission lines during a discharge sequence with powder injection: (a) Li-II emission, (b) W-I emission, and (c)  $D_\alpha$  emission.*

Real-time Li injection was also shown to reduce the W source from the walls, as measured by W-I line emission<sup>20</sup>. Fig. 7 shows a sequence of H-mode discharges in which real-time Li injection was introduced. The left-hand side panels in column (a) show the Li-II line emission, the central column (b) shows W-I line emission, and the right-hand side panels in column (c) show the divertor D<sub>a</sub> emission. The first discharge with Li powder injection, #70089, shows an immediate reduction of the W-I emission, indicative of a reduced sputtering source. The next three discharges #70090-#70092 maintain the low W-I line emission, while the last discharge #70093 shows that the low W-I emission is maintained despite no active Li injection. The reduced W-I emission can originate from multiple effects, including reduced heat flux to the W divertor PFCs due to enhanced radiation, and a coating effect of the W PFCs by the Li powder. The duration of this effect was not tested, but it is noted that the Li injection levels did not completely suppress ELMs in these discharges, i.e. ELM sputtering of the W from the PFCs was not eliminated *per se*.

Finally ELM triggering studies with a four-chamber Li granule injector showed (Fig. 8) a clear size threshold of  $\sim 500 \mu\text{m}$  for a near-unity ELM triggering probability<sup>21,22</sup>. This granule size threshold is remarkably similar to that observed in DIII-D<sup>23</sup>. The concept of a size threshold is predicted by theory<sup>24</sup>, and also from the simple consideration of a sufficient-sized perturbation in the steep gradient region to destabilize a pressure-driven instability. In addition, ELM pacing was also observed, but in these cases the paced ELM frequency of  $\sim 60\text{-}80 \text{ Hz}$  was below the natural ELM frequency between  $100\text{-}200 \text{ Hz}$ , which obviated ELM size mitigation experiments.

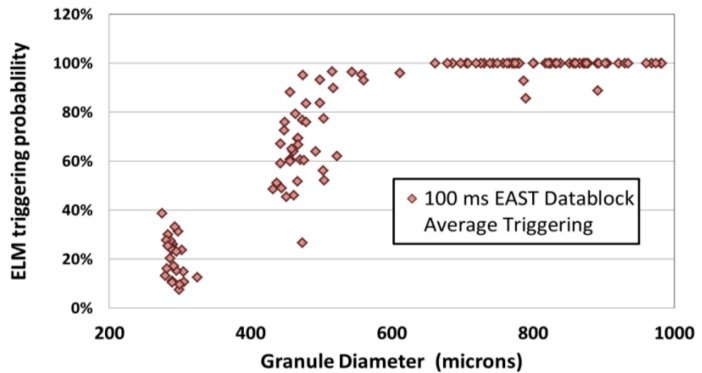


Fig. 8: ELM triggering probability vs. Li granule diameter for midplane injected granules at  $\sim 100 \text{ m/s}$  velocity, showing strong size threshold.

#### 4. SUMMARY AND CONCLUSIONS

The FLiLi limiter program has shown promising compatibility with H-mode discharges, even those heated with neutral beams and the accompanying fast ion population in the boundary plasma. While the FLiLi limiters showed good performance even when placed within 1 cm of the separatrix in RF heated discharges, the best performance in neutral beam heated discharges occurred with the limiter placed about 3 cm from the separatrix. The heating power and stored energy used in the generation 2 and 3 FLiLi limiter studies has been extended from the generation 1 experiments; this has been enabled by the continuous development of attractive scenarios with improving plasma performance and pulse length in EAST. In the next set of experiments, a test of a LIMIT-style FLiLi plate is planned, augmenting the gravity driven front surface flow with the TEMHD drive. Building on the success of the program, the extension of FLiLi science and technology to a future replacement of a small segment of the lower divertor is being evaluated.

We now have an existence proof of Li powder injection for ELM elimination with W PFCs, and also for W source reduction. The powder injection has a progressive conditioning effect at fixed injection rates. Future experiments will focus on extending the ELM elimination to higher power and lower collisionality discharges. In addition, we will investigate the use of larger Li particles, i.e. the size of Li granules injected for ELM triggering, in the gravitational dropper for wall conditioning. One of the limitations of small powder injection in future devices is the ability of the microscopic particles to penetrate close enough into the SOL to condition the divertor near high heat flux regions. Larger granules will naturally penetrate farther into the SOL of high-power discharges, and possibly overcome this limitation. For wall conditioning, we envision possible tangential injection of large Li granules into the SOL, i.e. far enough to penetrate near the separatrix but not into the pedestal region.

In the ELM triggering area, we have observed a granule size threshold as conceptually predicted by theory. Future experiments will focus on reproducing a robust low natural frequency ELMy H-mode for evaluation of

the effects of ELM pacing and heat flux mitigation. Such a scenario was recently obtained at EAST, and will be the target of the next set of experiments.

### ACKNOWLEDGEMENTS

This research was supported in part by the U.S. Dept. of Energy Contracts and Grants DE-AC02-09CH11466, DE-AC52-06NA25396, DE-AC05-00OR22725, DE-FC02-04ER54698, DE-SC0016915, DE-SC0016322, and DE-SC0016553, and in part by the National Key Research and Development Program of China under Contracts 2017YFA0402500 and 2017YFE0301100, the National Nature Science Foundation of China under Contract 11775261, 11625524, 11605246, 11075185 and 11021565. We gratefully acknowledge the contributions from the EAST technical staff.

### BIBLIOGRAPHY

1. B. Wan *et al.*, 2015 *Nucl. Fusion* **55** 104015
2. X. Gong *et al.*, 2017 *Plasma Science and Technology* **19** 032001
3. X. Gong *et al.*, 2017 *Bull. Am. Phys. Soc.* **62** BAPS.2017.DPP.TO4.1.
4. Z. Sun *et al.*, 2018 *Nucl. Mater. Energy* submitted
5. J. S. Hu *et al.*, 2016 *Nucl. Fusion* **56** 046011
6. G. Z. Zuo *et al.*, 2017 *Nucl. Fusion* **57** 046017
7. J. S. Hu *et al.*, 2018 *Nucl. Mater. Energy* submitted
8. J. Ren *et al.*, 2016 *Fusion Eng. Design* **102** 36
9. J. Ren *et al.*, 2015 *The Review of scientific instruments* **86** 023504
10. G. Z. Zuo *et al.*, 2017 *Rev. Sci. Instrum.* **88** 123506
11. G. Z. Zuo *et al.*, 2018 *Nucl. Fusion* submitted
12. R. Maingi *et al.*, 2018 *Nucl. Fusion* **58** 024003
13. R. Maingi *et al.*, 2012 *Nucl. Fusion* **52** 083001
14. D. Andruczyk *et al.*, 2017 *Fusion Science and Technology* **68** 497
15. D. N. Ruzic *et al.*, 2011 *Nucl. Fusion* **51** 102002
16. G. Z. Zuo *et al.*, 2012 *Plasma Phys. Control. Fusion* **54** 015014
17. J. S. Hu *et al.*, 2015 *Phys. Rev. Lett.* **114** 055001
18. P. T. Lang *et al.*, 2017 *Nucl. Fusion* **57** 016030
19. J. M. Canik *et al.*, 2018 *IEEE Trans. Plasma Sci.* **46** 1081
20. W. Xu *et al.*, 2018 *Fusion Eng. Design* at press
21. R. Lunsford *et al.*, 2018 *Nucl. Fusion* **58** 036007
22. Z. Sun *et al.*, 2018 *IEEE Trans. Plasma Sci.* **46** 1076
23. A. Bortolon *et al.*, 2016 *Nucl. Fusion* **56** 056008
24. G. T. A. Huijsmans *et al.*, 2015 *Phys. Plasmas* **22** 021805